IOP PUBLISHING CLASSICAL AND QUANTUM GRAVITY

Class. Quantum Grav. **26** (2009) 225015 (10pp) doi:10.1088/0264-9381/26/22/225015

Late-time tails of wave maps coupled to gravity

Piotr Bizoń[1], Tadeusz Chmaj[2,3], Andrzej Rostworowski[1] and Stanisław Zając[2]

[1] M. Smoluchowski Institute of Physics, Jagiellonian University, Kraków, Poland
[2] H. Niewodniczanski Institute of Nuclear Physics, Polish Academy of Sciences, Kraków, Poland
[3] Cracow University of Technology, Kraków, Poland

E-mail: bizon@th.if.uj.edu.pl

Received 17 June 2009, in final form 6 September 2009
Published 23 October 2009
Online at stacks.iop.org/CQG/26/225015

Abstract
We consider the late-time asymptotic behavior for solutions of Einstein's equations with the wave map matter. Using the third-order perturbation expansion about the flat spacetime we show that solutions starting from small compactly supported ℓ-equivariant initial data with $\ell \geqslant 1$ decay as $t^{-(2\ell+2)}$ at future timelike infinity and as $u^{-(\ell+1)}$ at future null infinity.

PACS numbers: 04.40.Nr, 04.25.Nx

1. Introduction

In this paper, we continue our investigations, initiated in [1], of the precise *quantitative* description of the late-time asymptotic behavior of self-gravitating massless fields. In [1] we considered the simplest case of a spherically symmetric massless scalar field. Using nonlinear perturbation analysis we showed that solutions starting from small initial data decay as t^{-3} at timelike infinity and as u^{-2} at null infinity. We also derived a simple analytic formula for the amplitude of the late-time tail in terms of initial data.

Here we study the analogous problem for wave maps which are a natural geometric generalization of the wave equation for the massless scalar field. This generalization seems interesting because in the so-called equivariant case the homotopy index ℓ of the map plays the role similar to the multipole index for spherical harmonics. However, in contrast to the decomposition of a scalar field into spherical harmonics which makes sense only at the linearized level, it is consistent to study nonlinear evolution for the wave map within a fixed equivariance class. In this sense ℓ-equivariant self-gravitating wave maps can serve as a poor man's toy-model of non-spherical collapse. The $\ell = 0$ case reduces to the spherically symmetric massless scalar field analyzed in [1] so hereafter we assume that $\ell \geqslant 1$. We note aside that the $\ell = 1$ case has been extensively studied in the past focusing on the critical behavior at the threshold of black hole formation [2–6]; however, to our knowledge, the late-time behavior of wave maps coupled to gravity has not been analyzed before.

Using the same third-order perturbation expansion about the flat spacetime as in [1] we show here that for small compactly supported initial data the late-time tail of the self-gravitating ℓ-equivariant wave map decays as $t^{-(2\ell+2)}$ at future timelike infinity and as $u^{-(\ell+1)}$ at future null infinity. We also compute the amplitude of the tail in terms of initial data. These analytic results are verified by the numerical integration of the Einstein wave map equations.

2. Setup

Let $U : \mathcal{M} \to \mathcal{N}$ be a map from a spacetime $(\mathcal{M}, g_{ab})$ into a Riemannian manifold $(\mathcal{N}, G_{AB})$. A pair (U, g_{ab}) is said to be a wave map coupled to gravity if it is a critical point of the action functional

$$S = \int_{\mathcal{M}} \left(\frac{R}{16\pi G} - \frac{\lambda}{2} g^{ab} \partial_a U^A \partial_b U^B G_{AB} \right) \mathrm{d}v, \tag{1}$$

where R is the scalar curvature of the metric g_{ab}, G is Newton's constant, λ is the wave map coupling constant and $\mathrm{d}v$ is the volume element on $(\mathcal{M}, g_{ab})$. The field equations derived from (1) are the Einstein equations $R_{ab} - \frac{1}{2} g_{ab} R = 8\pi G T_{ab}$ with the stress–energy tensor

$$T_{ab} = \lambda \left(\partial_a U^A \partial_b U^B - \tfrac{1}{2} g_{ab} (g^{cd} \partial_c U^A \partial_d U^B) \right) G_{AB}, \tag{2}$$

and the wave map equation

$$\Box_g U^A + \Gamma^A_{BC}(U) \partial_a U^B \partial_b U^C g^{ab} = 0, \tag{3}$$

where Γ^A_{BC} are the Christoffel symbols of the target metric G_{AB} and $\Box_g$ is the wave operator associated with the metric g_{ab}. As a target manifold we take the three-sphere with the round metric in polar coordinates $U^A = (F, \Theta, \Phi)$:

$$G_{AB}\, \mathrm{d}U^A\, \mathrm{d}U^B = \mathrm{d}F^2 + \sin^2 F (\mathrm{d}\Theta^2 + \sin^2\Theta\, \mathrm{d}\Phi^2). \tag{4}$$

For the four-dimensional spacetime $\mathcal{M}$ we assume spherical symmetry and use the following ansatz for the metric

$$g_{ab}\, \mathrm{d}x^a\, \mathrm{d}x^b = \mathrm{e}^{2\alpha(t,r)}(-\mathrm{e}^{2\beta(t,r)}\, \mathrm{d}t^2 + \mathrm{d}r^2) + r^2(\mathrm{d}\theta^2 + \sin^2\theta\, \mathrm{d}\phi^2). \tag{5}$$

In addition, we assume that the map U is spherically ℓ-equivariant, that is

$$F = F(t, r), \qquad (\Theta, \Phi) = \Omega_\ell(\theta, \phi), \tag{6}$$

where $\Omega_\ell : S^2 \to S^2$ is a harmonic eigenmap with eigenvalue $\ell(\ell + 1)$ (the components of Ω_ℓ are homogeneous harmonic polynomials of degree ℓ). Since the energy density of a harmonic eigenmap is constant [7], the energy–momentum tensor (2) for the ansatz (6) does not depend on angles and thus can be consistently coupled to the spherically symmetric Einstein equations. We note in passing that a very similar idea of introducing the 'angular momentum' into spherical collapse was put forward by Olabarrieta *et al* [8] in the context of critical phenomena. In terms of the mass function $m(t, r) = \dfrac{1}{2} r(1 - \mathrm{e}^{-2\alpha})$, the Einstein equations take the following form (hereafter primes and dots denote partial derivatives with respect to r and t, respectively):

$$m' = \frac{\kappa}{2} r^2\, \mathrm{e}^{-2\alpha}(F'^2 + \mathrm{e}^{-2\beta}\dot{F}^2) + \kappa \frac{\ell(\ell+1)}{2} \sin^2 F, \tag{7}$$

$$\dot{m} = \kappa\, r^2\, \mathrm{e}^{-2\alpha}\, \dot{F}\, F', \tag{8}$$

$$\beta' = \frac{2m}{r^2}\, \mathrm{e}^{2\alpha} - \kappa \ell(\ell+1)\, \mathrm{e}^{2\alpha} \frac{\sin^2 F}{r}, \tag{9}$$

where $\kappa = 4\pi G\lambda$ is a dimensionless parameter. The wave map equation (3) takes the form

$$(\mathrm{e}^{-\beta}\dot{F})^{\cdot} - \frac{1}{r^2}(r^2\,\mathrm{e}^{\beta}F')' + \mathrm{e}^{\beta+2\alpha}\ell(\ell+1)\frac{\sin 2F}{2r^2} = 0. \tag{10}$$

For $\ell = 0$ the above equations reduce to the Einstein-massless scalar field equations analyzed by us in [1]. For $\kappa = 0$ (no gravity), equations (7)–(9) are trivially solved by $m = 0$ and $\beta = 0$, while equation (10) reduces to the flat space wave map equation.

3. Iterative scheme

We assume that initial data are small, smooth and compactly supported (the last assumption can be replaced by a suitable fall-off condition):

$$F(0,r) = \varepsilon g(r), \qquad \dot{F}(0,r) = \varepsilon h(r). \tag{11}$$

We make the following perturbative expansion:

$$m(t,r) = m_0(t,r) + \varepsilon m_1(t,r) + \varepsilon^2 m_2(t,r) + \cdots, \tag{12}$$

$$\beta(t,r) = \beta_0(t,r) + \varepsilon\beta_1(t,r) + \varepsilon^2\beta_2(t,r) + \cdots, \tag{13}$$

$$F(t,r) = F_0(t,r) + \varepsilon F_1(t,r) + \varepsilon^2 F_2(t,r) + \varepsilon^3 F_3(t,r) + \cdots. \tag{14}$$

Substituting this expansion into the field equations and grouping terms with the same power of ε we get the iterative scheme which can be solved recursively.

We consider perturbations about Minkowski spacetime, so $m_0 = \beta_0 = F_0 = 0$. At the first order, the metric functions $m_1 = \beta_1 = 0$ (this follows from regularity at $r = 0$), while F_1 satisfies the flat space radial wave equation for the ℓth spherical harmonic:

$$\Box_{(\ell)}F_1 = 0, \qquad \Box_{(\ell)} = \partial_t^2 - \partial_r^2 - \frac{2}{r}\partial_r + \frac{\ell(\ell+1)}{r^2}, \tag{15}$$

with initial data $F_1(0,r) = g(r)$, $\dot{F}_1(0,r) = h(r)$. The general everywhere regular solution of equation (15) is given by a superposition of outgoing and ingoing waves:

$$F_1(t,r) = F_1^{\mathrm{ret}}(t,r) + F_1^{\mathrm{adv}}(t,r), \tag{16}$$

where

$$\begin{aligned} F_1^{\mathrm{ret}}(t,r) &= \frac{1}{r}\sum_{k=0}^{l}\frac{(2\ell-k)!}{k!(\ell-k)!}\frac{a^{(k)}(u)}{(v-u)^{\ell-k}}, \\ F_1^{\mathrm{adv}}(t,r) &= \frac{1}{r}\sum_{k=0}^{\ell}(-1)^{k+1}\frac{(2\ell-k)!}{k!(\ell-k)!}\frac{a^{(k)}(v)}{(v-u)^{\ell-k}} \end{aligned} \tag{17}$$

and $u = t - r$ and $v = t + r$ are the retarded and advanced times, respectively (the superscript in parentheses denotes the kth derivative). Note that for compactly supported initial data, the generating function $a(x)$ can be chosen to have compact support as well (this condition determines $a(x)$ uniquely).

At the second order $\Box_{(\ell)}F_2 = 0$, hence $F_2 = 0$ (because it has zero initial data), while the metric functions satisfy the following equations:

$$m_2' = \frac{\kappa}{2}r^2\left(\dot{F}_1^2 + F_1'^2 + \frac{\ell(\ell+1)}{r^2}F_1^2\right), \tag{18}$$

$$\dot{m}_2 = \kappa\, r^2\dot{F}_1F_1', \tag{19}$$

$$\beta_2' = \frac{2m_2}{r^2} - \kappa\frac{\ell(\ell+1)}{r}F_1^2. \tag{20}$$

We temporarily postpone the discussion of this system and proceed now to the third order, where we have

$$\Box_{(l)}F_3 = 2\beta_2\ddot{F}_1 + \dot{\beta}_2\dot{F}_1 + \beta_2'F_1' - \frac{2\ell(\ell+1)m_2F_1}{r^3} + \frac{2\ell(\ell+1)F_1^3}{3r^2}. \tag{21}$$

To solve this equation, we use the Duhamel formula for the solution of the inhomogeneous wave equation $\Box_{(\ell)}F = N(t,r)$ with zero initial data:

$$F(t,r) = \frac{1}{2r}\int_0^t \mathrm{d}\tau \int_{|t-r-\tau|}^{t+r-\tau} \rho P_\ell(\mu)N(\tau,\rho)\,\mathrm{d}\rho, \tag{22}$$

where $P_\ell(\mu)$ are Legendre polynomials of degree ℓ and $\mu = (r^2+\rho^2-(t-\tau)^2)/2r\rho$ (note that $-1 \leqslant \mu \leqslant 1$ within the integration range). Applying this formula to equation (21), using null coordinates $\eta = \tau - \rho$ and $\xi = \tau + \rho$, and the abbreviation $K(m,\beta,F) = 2\beta\ddot{F} + \dot{\beta}\dot{F} + \beta'F' - (2\ell(\ell+1)/r^2)(mF/r - F^3/3)$, we obtain

$$F_3(t,r) = \frac{1}{8r}\int_{|t-r|}^{t+r}\mathrm{d}\xi\int_{-\xi}^{t-r}(\xi-\eta)P_\ell(\mu)K(m_2(\xi,\eta),\beta_2(\xi,\eta),F_1(\xi,\eta))\,\mathrm{d}\eta, \tag{23}$$

where now $\mu = (r^2+(\xi-t)(t-\eta))/r(\xi-\eta)$. If the initial data (11) vanish outside a ball of radius R, then for $t > r+R$ we may drop the advanced part of $F_1(t,r)$ and interchange the order of integration in (23) to get

$$F_3(t,r) = \frac{1}{8r}\int_{-\infty}^{\infty}\mathrm{d}\eta\int_{t-r}^{t+r}(\xi-\eta)P_\ell(\mu)K(m_2(\xi,\eta),\beta_2(\xi,\eta),F_1^{\mathrm{ret}}(\xi,\eta))\,\mathrm{d}\xi. \tag{24}$$

In order to determine the late-time behavior of $F_3(t,r)$, we need to know the behavior of the source term K along the light cone for large values of r (the intersection of the integration range in (24) with the support of $F_1^{\mathrm{ret}}(t,r)$). Having that, we shall expand the function K in (24) in the inverse powers of $\rho = (\xi-\eta)/2$ and calculate the integrals using the following identity (see the appendix in [9] for the derivation):

$$\int_{t-r}^{t+r}\mathrm{d}\xi\,\frac{P_\ell(\mu)}{(\xi-\eta)^n} = (-1)^l\frac{2(n-2)^{\underline{\ell}}}{(2\ell+1)!!}\frac{r^{\ell+1}(t-\eta)^{n-\ell-2}}{[(t-\eta)^2-r^2]^{n-1}}F\left(\begin{matrix}\frac{\ell+2-n}{2},\ \frac{\ell+3-n}{2}\\ \ell+3/2\end{matrix}\,\middle|\,\left(\frac{r}{t-\eta}\right)^2\right), \tag{25}$$

where $(n-2)^{\underline{\ell}} = (n-2)(n-3)\cdots(n-\ell-1)$.

Now, we return to the analysis of the second-order equations (18)–(20). Substituting the outgoing solution (17) into (18) and integrating, we get

$$\begin{aligned} m_2(t,r) \overset{t>R}{=} \kappa\int_0^r\Bigg[&(a^{(\ell+1)}(t-\rho))^2 - \sum_{1\leqslant k\leqslant 2\ell+2}\ \sum_{0\leqslant n\leqslant k-1}\\ &\times\frac{(\ell+n)^{\underline{2n}}(\ell+k-1-n)^{\underline{2(k-1-n)}}(\ell^2+\ell+(k-n)(n+1))}{k2^k\,(k-1-n)!\,n!}\\ &\times\partial_\rho\frac{a^{(\ell+1+n-k)}(t-\rho)\,a^{(\ell-n)}(t-\rho)}{\rho^k}\Bigg]\mathrm{d}\rho, \end{aligned} \tag{26}$$

where we used that $m_2(t,r=0)=0$, which follows from regularity of initial data at the origin and (19). Here and in the following, we use repeatedly the fact that $a(x)=0$ for $|x|>R$, R being the radius of a ball on which the initial data (11) are supported. To describe the behavior

of $m_2(t,r)$ along the lightcone, it is convenient to use the null coordinate $u = t - r$ instead of t, and rewrite (26) as

$$m_2(u,r) \overset{r+u>R}{=} \kappa \left[\int_u^\infty (a^{(\ell+1)}(s))^2 \,\mathrm{d}s - \frac{\ell^2+\ell+1}{2r}(a^{(\ell)}(u))^2 - \frac{\ell(\ell+1)(\ell^2+\ell+2)}{4} \frac{a^{(\ell-1)}(u)a^{(\ell)}(u)}{r^2} + \mathcal{O}\left(\frac{1}{r^3}\right)\right]. \tag{27}$$

Next, using the gauge freedom to set $\beta_2(t, r=0) = 0$ and integrating equation (20), we get

$$\beta_2(t,r) \overset{t\geq R}{=} 2\kappa \int_0^r \frac{1}{\rho^2} \int_{t-\rho}^\infty (a^{(\ell+1)}(s))^2 \,\mathrm{d}s\,\mathrm{d}\rho - \kappa \int_0^r \left[(2\ell^2+2\ell+1) \frac{(a^{(\ell)}(t-\rho))^2}{\rho^3} + \frac{\ell(\ell+1)(3\ell^2+3\ell+2)}{2} \frac{a^{(\ell-1)}(t-\rho)a^{(\ell)}(t-\rho)}{\rho^4} + \mathcal{O}\left(\frac{1}{\rho^5}\right)\right] \mathrm{d}\rho. \tag{28}$$

The first integral can be integrated by parts giving

$$\beta_2(u,r) \overset{r+u>R}{=} 2\kappa \left[-\frac{1}{r} \int_u^\infty \left(a^{(\ell+1)}(s)\right)^2 \,\mathrm{d}s + \int_u^\infty \frac{(a^{(\ell+1)}(s))^2}{r-(s-u)} \,\mathrm{d}s \right] - \kappa \int_u^\infty \left[(2\ell^2+2\ell+1) \frac{(a^{(\ell)}(s))^2}{(r-(s-u))^3} + \frac{\ell(\ell+1)(3\ell^2+3\ell+2)}{2} \frac{a^{(\ell-1)}(s)a^{(\ell)}(s)}{(r-(s-u))^4} \right] \mathrm{d}s + \mathcal{O}\left(\frac{1}{r^5}\right). \tag{29}$$

4. Tails

Now, we shall apply the method described above to compute the late-time asymptotics of solutions in the third-order approximation. Hereafter, it is convenient to define the following integrals (for non-negative integers m, n):

$$I_n^m(u) = \int_u^\infty (s-u)^m (a^{(n)}(s))^2 \mathrm{d}s. \tag{30}$$

4.1. $\ell = 1$

From (29) we have

$$\beta_2(u,r) \overset{r+u>R}{=} \frac{\kappa}{r^2}\left[2I_2^1(u) + \frac{1}{r}\left(2I_2^2(u) - 5I_1^0(u)\right) + \mathcal{O}\left(\frac{1}{r^2}\right)\right], \tag{31}$$

$$\dot{\beta}_2(u,r) \overset{r+u>R}{=} -\frac{\kappa}{r^2}\left[2I_2^0(u) + \frac{1}{r}\left(4I_2^1(u) - 5(a'(u))^2\right) + \mathcal{O}\left(\frac{1}{r^2}\right)\right], \tag{32}$$

$$\beta_2'(u,r) \overset{r+u>R}{=} \frac{\kappa}{r^2}\left[2I_2^0(u) - \frac{5}{r}(a'(u))^2 + \mathcal{O}\left(\frac{1}{r^2}\right)\right]. \tag{33}$$

Substituting (17) and (31)–(33) into (24) we obtain

$$F_3(t,r) = \frac{4\kappa}{r} \int_{-\infty}^{+\infty} \mathrm{d}\eta \int_{t-r}^{t+r} \mathrm{d}\xi \, \frac{P_1(\mu)}{(\xi-\eta)^2} \left[\frac{\mathrm{d}}{\mathrm{d}\eta}\left(I_2^1(\eta)a''(\eta)\right) - \frac{1}{\xi-\eta}\left(I_2^1(\eta)a'(\eta) - \frac{\mathrm{d}}{\mathrm{d}\eta}U_1(\eta)\right) + \mathcal{O}\left(\frac{1}{(\xi-\eta)^2}\right)\right], \tag{34}$$

where

$$U_1(\eta) = 4I_2^1(\eta)a'(\eta) + \big(2I_2^2(\eta) - 5I_1^0(\eta)\big)a''(\eta). \tag{35}$$

Performing the inner integral over ξ in (34) with the help of the identity (25) we get the asymptotic behavior which is valid for large retarded times u :

$$F_3(t,r) = \frac{r}{(t^2-r^2)^2}\left[\kappa A_1 + \mathcal{O}\left(\frac{t}{t^2-r^2}\right)\right], \tag{36}$$

where

$$A_1 = \frac{8}{3}\int_{-\infty}^{+\infty} (a''(s))^2 a(s)\,\mathrm{d}s. \tag{37}$$

From (36), we obtain the late-time tails in both asymptotic regimes: $F_3(t,r) \simeq \kappa A_1 r t^{-4}$ at future timelike infinity ($r = \text{const}$, $t \to \infty$) and $(rF_3)(v=\infty,u) \simeq \kappa A_1 (2u)^{-2}$ at future null infinity ($v=\infty$, $u\to\infty$).

4.2. $\ell \geqslant 2$

We give the detailed calculation only for $\ell = 2$. In this case, we have from (29)

$$\beta_2(u,r) \overset{r+u>R}{=} \frac{\kappa}{r^2}\left[2I_3^1(u) + \frac{1}{r}\big(2I_3^2(u) - 13I_2^0(u)\big) + \frac{1}{r^2}\big(2I_3^3(u) - 39I_2^1(u) + 30(a'(u))^2\big) + \mathcal{O}\left(\frac{1}{r^3}\right)\right], \tag{38}$$

$$\dot\beta_2(u,r) \overset{r+u>R}{=} -\frac{\kappa}{r^2}\left[2I_3^0(u) + \frac{1}{r}\big(4I_3^1(u) - 13(a''(u))^2\big) + \frac{1}{r^2}\big(6I_3^2(u) - 39I_2^0(u) - 60a'(u)a''(u)\big) + \mathcal{O}\left(\frac{1}{r^3}\right)\right], \tag{39}$$

$$\beta_2'(u,r) \overset{r+u>R}{=} \frac{\kappa}{r^2}\left[2I_3^0(u) - \frac{13}{r}(a''(u))^2 - \frac{60}{r^2}a'(u)a''(u) + \mathcal{O}\left(\frac{1}{r^3}\right)\right]. \tag{40}$$

Substituting (17) and (38)–(40) into (24) we obtain

$$F_3(t,r) = \frac{4}{r}\int_{-\infty}^{+\infty}\mathrm{d}\eta\int_{t-r}^{t+r}\mathrm{d}\xi\,\frac{P_l(\mu)}{(\xi-\eta)^2}\Bigg[\kappa\frac{\mathrm{d}}{\mathrm{d}\eta}\left(I_3^1(\eta)a^{(3)}(\eta)\right) + \frac{\kappa}{\xi-\eta} \times\left(-5I_3^0(\eta)a''(\eta) + \frac{\mathrm{d}}{\mathrm{d}\eta}U_2(\eta)\right) + \frac{4}{(\xi-\eta)^2}\Bigg((a''(\eta))^3 + 2\kappa\Bigg(2(a''(\eta))^3 - 3(a^{(3)}(\eta))^2 a(\eta) + \frac{1}{8}\frac{\mathrm{d}}{\mathrm{d}\eta}V_2(\eta)\Bigg)\Bigg) + \mathcal{O}\left(\frac{1}{(\xi-\eta)^3}\right)\Bigg], \tag{41}$$

where

$$U_2(\eta) = 8I_3^1(\eta)a''(\eta) + \big(2I_3^2(\eta) - 13I_2^0(\eta)\big)a^{(3)}(\eta) \tag{42}$$

and

$$V_2(\eta) = -24I_3^0(\eta)a(\eta) + 36I_3^1(\eta)a'(\eta) + \big(-117I_2^0(\eta) + 18I_3^2(\eta)\big)a''(\eta) + \big(-78I_2^1(\eta) + 4I_3^3(\eta) + 60(a'(\eta))^2\big)a^{(3)}(\eta). \tag{43}$$

Performing the inner integral over ξ in (41) with the help of the identity (25) we get the asymptotic behavior for large retarded times:

$$F_3(t,r) = \frac{r^2}{(t^2-r^2)^3}\left[\kappa A_2 + B_2 + \mathcal{O}\left(\frac{t}{t^2-r^2}\right)\right], \tag{44}$$

where

$$A_2 = \frac{128}{15}\int_{-\infty}^{+\infty}[2(a''(s))^3 - 3(a^{(3)}(s))^2 a(s)]\,\mathrm{d}s \quad \text{and} \quad B_2 = \frac{64}{15}\int_{-\infty}^{+\infty}(a''(s))^3\,\mathrm{d}s. \tag{45}$$

For the general ℓ it is easy to see that the first nonzero contribution to the tail comes from the term with $n = \ell + 2$ in the identity (25) which gives the following asymptotics:

$$F_3(t,r) = \frac{r^\ell}{(t^2-r^2)^{\ell+1}}\left[\kappa A_\ell + B_\ell + \mathcal{O}\left(\frac{t}{t^2-r^2}\right)\right]. \tag{46}$$

Formula (46) gives the first term in the asymptotic series approximation of the solution for late retarded times, that is for small ε we have

$$\frac{(t^2-r^2)^{\ell+1}}{r^\ell}|F(t,r) - \varepsilon^3 F_3(t,r)| = \mathcal{O}(\varepsilon^5). \tag{47}$$

We have not attempted to derive a general formula for the coefficients A_ℓ and B_ℓ—the computation of these coefficients for each given ℓ is straightforward but as ℓ increases the algebra becomes tedious since it involves high-order expansions of the metric functions along the light cone. Anyway, it follows from (46) that the tail behaves as $F_3(t,r) \sim r^\ell t^{-(2\ell+2)}$ at future timelike infinity and as $(rF_3)(v=\infty,u) \sim u^{-(\ell+1)}$ at future null infinity.

Remark 1. For $\ell \geqslant 2$ the tail (46) has two parts quantified by the coefficients κA_ℓ and B_ℓ, respectively. The A_ℓ-part comes from the gravitational self-interaction of the wave map and vanishes for $\kappa = 0$. The B_ℓ-part comes from the cubic nonlinearity of the wave map equation and is present without gravity as well. The case $\ell = 1$ is special in the sense that the B_ℓ-part is absent in (36) since it is subdominant (decaying as t^{-5}) with respect to the leading order term.

Remark 2. It is instructive to compare the tail (46) with the tail for a test linear massless field propagating on a fixed stationary asymptotically flat background. According to the Price law [10–12] the ℓth multipole of this linear tail $\phi_\ell(t,r) \sim r^\ell t/(t^2-r^2)^{\ell+2}$ for $t-r \to \infty$. This decay is by one power faster than that in (46). Of course, this difference is not very surprising as the tail studied here and Price's tail correspond to different physical situations; however, we point it out as another example of the inapplicability of linearized theory in the study of radiative relaxation processes (see [13, 14] for other examples). We shall discuss this issue in more detail elsewhere [15].

Remark 3. It is worth stressing that formula (46) does not apply to the case $\ell = 0$ corresponding to the massless scalar field which decays as $t/(t^2-r^2)^2$ [1].

5. Numerics

In this section, we compare the above analytic predictions with the results of numerical solutions of the Einstein wave map equations (7)–(10) for various initial data. The details of the numerical method were given in [1] for the case $\ell = 0$. The only difference for higher ℓ is the boundary condition $F(t,r) \sim r^\ell$ for small r which guarantees regularity at the origin. The initial data were generated by the Gaussian

$$\varepsilon a(x) = \varepsilon \exp(-x^2) \tag{48}$$

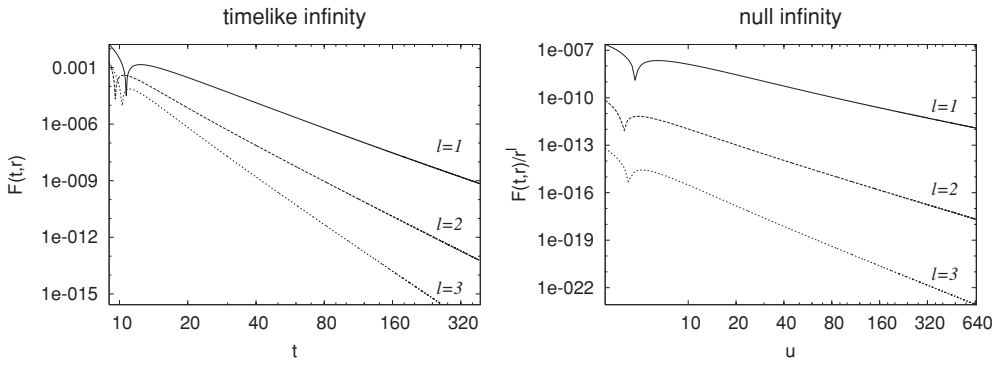

Figure 1. Left panel: the log–log plot of $F(t,r)$ for fixed $r = 5$. Fitting (51) we get power-law exponents $\gamma = -4.0196$ ($\ell = 1$), -6.0009 ($\ell = 2$), -8.0049 ($\ell = 3$), in agreement with the analytic prediction (46). Right panel: the log–log plot of $F(t, r)/r^{\ell}$ for fixed large advanced time $v = t + r = 1200$ as the function of retarded time $u = t - r$. The analogous fit to (51) yields the exponents -2.0036 ($\ell = 1$), -3.0004 ($\ell = 2$), -4.0095 ($\ell = 3$), in accordance with (46). In both panels $\kappa = 0.02$ and $\varepsilon = 2.0$ ($\ell = 1$), $\varepsilon = 0.7$ ($\ell = 2$), $\varepsilon = 0.3$ ($\ell = 3$).

Table 1. The comparison of analytic and numerical amplitudes of the tails at timelike infinity. Here $\kappa = 0.02$ and $r = 5$. The third-order approximation reads $A = \varepsilon^3 \kappa r A_1$ for $\ell = 1$ and $A = \varepsilon^3 r^2(\kappa A_2 + B_2)$ for $\ell = 2$.

	$A(\ell = 1)$			$A(\ell = 2)$	
ε	Theory	Numerics	ε	Theory	Numerics
0.05	9.096×10^{-5}	9.051×10^{-5}	0.05	−0.072 77	−0.072 74
0.1	7.277×10^{-4}	7.289×10^{-4}	0.1	−0.582 16	−0.584 76
0.4	0.046 57	0.047 01	0.2	−4.657 27	−4.6841
0.8	0.372 58	0.374 14	0.4	−37.2582	−37.3778
2.4	10.0597	10.0299	0.65	−159.875	−160.441
3.2	23.8452	16.0528	0.7	−199.681	−189.377
3.8	39.9303	19.6931	0.75	−245.598	−189.792

for different values of ε. For these initial data, formula (37) gives for $\ell = 1$

$$A_1 = \frac{64}{27}\sqrt{3\pi} \approx 7.2769, \tag{49}$$

and formula (45) gives for $\ell = 2$

$$A_2 = -\frac{10240}{81}\sqrt{3\pi} \approx -388.1, \qquad B_2 = -\frac{2048}{405}\sqrt{3\pi} \approx -15.52. \tag{50}$$

In order to extract the parameters of the tails at timelike infinity, we fit our numerical data with the formula

$$F(t, r) = At^{\gamma} \exp(B/t + C/t^2). \tag{51}$$

The results and their confrontation with analytic predictions are summarized in table 1 and figures 1, 2 and 3. From this comparison we conclude that the third-order approximation is excellent for sufficiently small initial data. For large data approaching the black-hole threshold the third-order approximation breaks down—this is seen in figure 2 as the deviation from the scaling $A \sim \varepsilon^3$ and in figure 3 as the deviation from the linear dependence of A on κ.

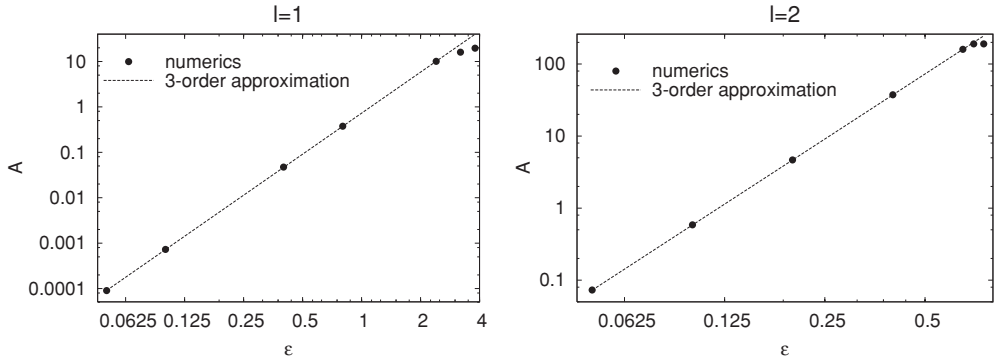

Figure 2. The log–log plot of the amplitude of the tail at timelike infinity as a function of the amplitude of initial data (black dots) for fixed $\kappa = 0.02$ and $r = 5$. The third-order approximation (dashed line) is excellent for small data, but it breaks down for large data lying near the threshold of black hole formation.

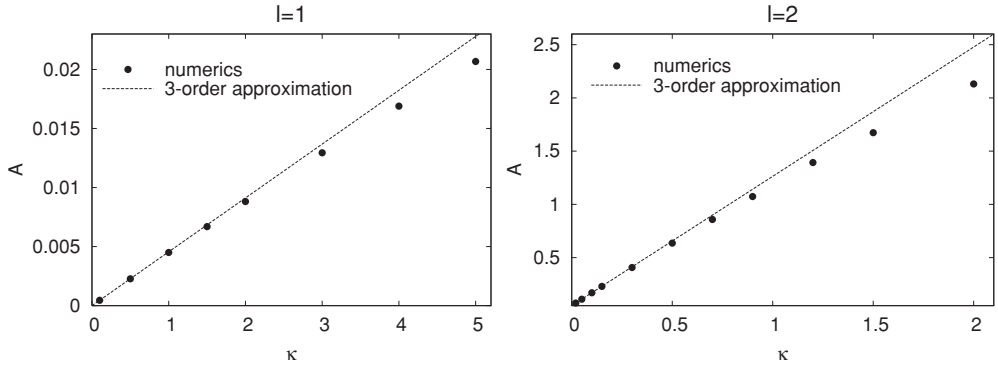

Figure 3. The plot of the amplitude of the tail at timelike infinity as a function of the coupling constant κ (black dots) for fixed $\varepsilon = 0.05$ and $r = 5$. As κ increases we leave the small-data regime and consequently the third-order approximation (dashed line) deteriorates.

It should be emphasized that we get the same decay rates $t^{-(2\ell+2)}$ (at timelike infinity) and $u^{-(\ell+1)}$ (at null infinity) for *all* subcritical evolutions, regardless of whether our third-order formula reproduces accurately the amplitude of the tail (for small data) or fails (for large data).

Acknowledgments

We acknowledge support by the MNII grants: NN202 079235 and 189/6.PRUE/2007/7.

References

[1] Bizoń P, Chmaj T and Rostworowski A 2009 *Class. Quantum Grav.* **26** 175006
[2] Bizoń P and Wasserman A 2000 *Phys. Rev.* D **62** 084031
[3] Husa S *et al* 2000 *Phys. Rev.* D **62** 104007
[4] Lechner Ch *et al* 2002 *Phys. Rev.* D **65** 081501
[5] Bizoń P and Wasserman A 2002 *Class. Quantum Grav.* **19** 3309

[6] Aichelburg P, Bizoń P and Tabor Z 2006 *Class. Quantum Grav.* **23** S299
[7] Eells J and Ratto A 1993 *Harmonic Maps and Minimal Immersions with Symmetries Annals of Mathematical Studies* vol 130 (Princeton, NJ: Princeton University Press)
[8] Olabarrieta I *et al* 2007 *Phys. Rev.* D **76** 124014
[9] Bizoń P, Chmaj T and Rostworowski A 2008 *Phys. Rev.* D **78** 024044
[10] Price R H 1972 *Phys. Rev.* D **5** 2419
[11] Gundlach C, Price R and Pullin J 1994 *Phys. Rev.* D **49** 883
[12] Poisson E 2002 *Phys. Rev.* D **66** 044008
[13] Bizoń P, Chmaj T and Rostworowski A 2007 *Phys. Rev.* D **76** 124035
[14] Bizoń P, Chmaj T and Rostworowski A 2007 *Class. Quantum Grav.* **24** F55
[15] Bizoń P and Rostworowski A 2009 in preparation